X-ray and Monte Carlo studies on the 19°C transition of poly(tetrafluoroethylene)

Takashi Yamamoto and Tetsuhiko Hara
Department of Physics, Faculty of Science, Yamaguchi University, Yamaguchi, Japan
(Received 19 July 1985; revised 17 September 1985)

The 19°C transition of poly(tetrafluoroethylene) (PTFE) from the low temperature phase II to the high temperature phase IV is investigated by X-ray diffraction and Monte Carlo (MC) methods. The change in the chain packing around the transition point is examined carefully by separating the very close reflections on the equator. The conventional unit cell parameters a and γ show abrupt changes at 19°C from $a=5.61$ Å and $\gamma=119.3°$ (pseudohexagonal) to $a=5.67$ Å and $\gamma=120.0°$ (hexagonal), indicating a sharp first order transition. The change is ascribed to a dilatation of the spacing that occurs predominantly in one direction $[\bar{1},1]$. The rotational motion of the chains around the chain axes in phase II is examined in the vicinity of the transition point through the temperature dependence of a reflection on the second layer line. No evident increase in the rotational motion around the chain axis can be detected up to the transition point, which is again indicative of a clear first order nature of the transition. The chain packings in phases II and IV are simulated by the MC method used in our previous paper. It is shown that phases II and IV show marked differences in their chain packings. Details of the 19°C transition are discussed on the basis of these simulated structures.

(Keywords: Monte Carlo simulation; poly(tetrafluoroethylene); X-ray diffraction; transition)

INTRODUCTION

Poly(tetrafluoroethylene) (PTFE) is a unique polymer having many crystalline phases namely I, II, III, IV, and I'[1]. Transitions among these phases are reversible, and are accompanied by changes in chain conformation as well as chain packing. They have attracted the attention of many workers owing to interesting aspects concerning their molecular mechanisms[1-11].

The transition from the phase II to the phase IV at 19°C at atmospheric pressure has been much studied since the early work by Bunn and Howells[2-7,9]. Below 19°C, the crystal lattice is triclinic with a unit cell composed of two chain stems of opposite helical sense having approximately 13/6 conformation[12-14]. With increasing temperature, the rotational disorder of the chains is enhanced around the chain axes, and the crystal transforms to the disordered phase IV at 19°C.

Detailed inspection shows, however, that the nature of the 19°C transition is quite obscure. A definite thermal hysteresis was observed in the volume–temperature curve measured by Quinn *et al.*[2], which suggested the transition to be a first order one. However, the result of the specific heat measurement seems to suggest a second order transition[4]. The usual picture that the molecular oscillation around the chain axis increases near the transition point also suggests the transition to be of a second order nature. It is now evident that the transition is of an order–disorder type. However, it is uncertain what is the order parameter; the degree of freedom responsible for the order–disorder phenomenon is not obvious. Recent structural studies of the phase II showed that there is an ordered mixed array of the right handed and the left handed helices in the phase II[12-14]. Therefore the rotational order, which has been of major interest in previous works, is not the only candidate for the order parameter. We must also consider the order in the arrangement of the right handed and the left handed helices.

The aim of the present paper is to re-examine the 19°C transition by X-ray diffraction and Monte Carlo (MC) simulation taking into account recent knowledge of the crystal structure of the low temperature phase II.

X-RAY DIFFRACTION

A fibre sample of PTFE was used for the X-ray diffraction measurement after annealing, kept at constant length, in a silicone oil bath at about 250°C for one day. The sample, which was held by a metal sample holder, was cooled by blowing cold N_2 gas from liquid N_2. The temperature of the sample was controlled to within ± 0.5°C by adjusting the amount of cold N_2 gas. Line-focussed (for equatorial and meridional reflections) or point-focussed (for the second layer reflections) X-ray beam (CuKα) was transmitted symmetrically through the sample. In order to resolve very close reflections on the equator and the meridian, we used a severly collimated system (a half width of 000 reflection of about 0.06°), thin samples (about 0.1 mm thick), a fine focussed X-ray source, and reflections at angles as high as possible. The intensity measurement of the reflections was made using a scintillation counter and a goniometer with step scan facility controlled by a microcomputer. Monochromatization was effected using a Ni filter and a pulse height analyser.

MONTE CARLO METHOD

The MC calculation method and the van der Waals potentials used were the same as those used in our

0032-3861/86/070986-07$03.00

previous papers[14,15]. In the present work, MC calculations for the phases II and IV were done. It was assumed that the chain took the 13/6 and 15/7 helical conformations in the phases II and IV, respectively. Lattice parameters and temperatures used in the present calculations for the phases II and IV, and numbers of the relevant figures are listed in *Table 1*. In our previous paper on the phase II[14], the chains were simply assumed to be packed in a hexagonal lattice. Here we recalculate the structure of the phase II, taking the pseudohexagonal nature of the lattice into account. Both the right-hand chains (hereafter abbreviated as the R-chains) and the left-handed chains (hereafter abbreviated as the L-chains) were assumed to have 13 and 15 possible orientations in the phases II and IV, respectively. The size of the lattice is limited to 50×50 with periodic boundary conditions.

RESULTS AND DISCUSSION

X-ray diffraction results

Figure 1 shows the changes in profiles in the equatorial reflections around $2\theta = 32°$. Below 10°C, the reflection is a doublet with relative integrated intensities of about 1:2. The multiplicities of the 110 and $2\bar{1}0$ reflections of the hexagonal lattice are 2 and 4, respectively, and the structure factors of the two reflections in PTFE crystal are considered to be almost equal. Therefore, the lower and higher angle peaks are considered simply as the 110 and $2\bar{1}0$ reflections of the phase II, respectively. *Figure 2* shows a schematic picture of the chain packing, where the circles in the Figure represent chain molecules viewed along the chain axis. Conventional unit cell parameters a and γ, and the (110) and $(2\bar{1}0)$ planes are depicted. Directions [1,0], [1,1], and [0,1] are simply denoted as I, II, and III directions, respectively. As can be seen in *Figure 1*, the intensity of the higher angle peak decreases whereas that of the lower angle peak increases with the increase in temperature. The multiplicities of the 110 and $2\bar{1}0$ reflections of the phase II must be maintained until the transition to the phase IV at 19°C. Above 10°C, therefore, the lower angle peak should be considered to be a superposition of the 110 reflections of the phase II and the phase IV, whereas the higher angle peak is the $2\bar{1}0$ reflection of the phase II. Above 19°C, only the 110 reflection of the phase IV can be observed. By separating the apparent diffraction profile *Figure 1* into two Gaussian functions by the least-squares-method (SALS)[16], the peak positions, peak heights, and integrated intensities of the two peaks were determined. *Figure 3* shows the changes in the integrated intensities of the two peaks. Below 10°C, relative intensities of the two peaks are 0.48:1. In the Figure, the intensity of the 110 reflection of the phase IV is also shown, which was estimated by subtracting 0.48 times the intensity of the $2\bar{1}0$ reflection of the phase II (higher angle peak) from the intensity of the lower angle peak. It is well known that the rotational

Table 1 Lattice parameters and temperatures used for the calculations, and the numbers of the figures of the resulting patterns.

Phase	$a(=b)$ (Å)	γ (degrees)	T(K)	Figure
II	5.65	119.3	50	10(a),12(a)
II	5.65	119.3	300	10(a),12(b)
IV	5.75	120.0	300	13,14

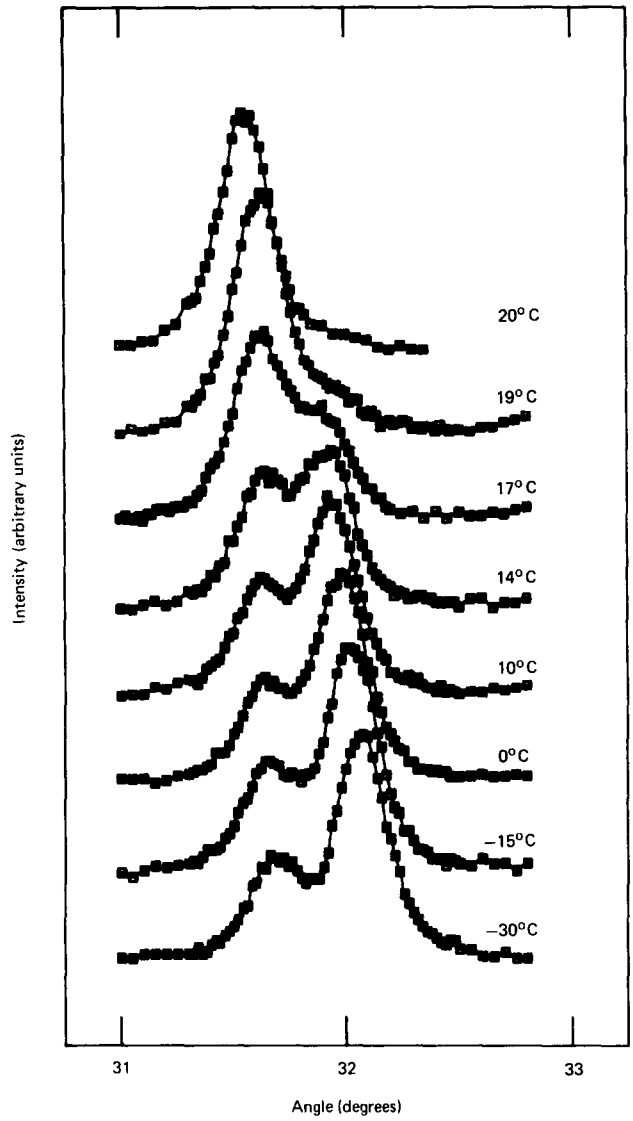

Figure 1 Diffraction profiles of equatorial reflections around $2\theta = 32°$ at various temperatures. Curves are shifted upward with increasing temperature

motion of the chains does not lead to a decrease in the intensities of the equatorial reflections[7]. The increase in the translational motion of the chains in the directions perpendicular to the chain axis near 19°C may contribute to the observed intensity decrease of the equatorial reflections of the phase II. However, since the decrease in the intensity of the $2\bar{1}0$ reflection of the phase II and the increase in that of the 110 reflection of the phase IV are quite compensating, the changes in the intensities are considered as due to changes in the fractions of the phases II and IV. *Figure 3* shows that the fraction of the phase II decreases abruptly between 10°C and 19°C, accompanied by a rapid increase in that of the phase IV.

Figure 4 shows temperature dependence of the spacings $d(110)$ and $d(2\bar{1}0)$ determined from the peak positions of the apparent two peaks. Below 10°C, both spacings increase linearly with temperature. Since the complicated effects of the phase IV on the profiles of the two peaks can be neglected below 10°C, the linear increase in the spacings can be attributable to the thermal expansion of the phase II. Above 10°C, the higher angle peak becomes smaller, especially near 19°C, and the lower angle peak becomes a superposition of the 110 reflections of phases II

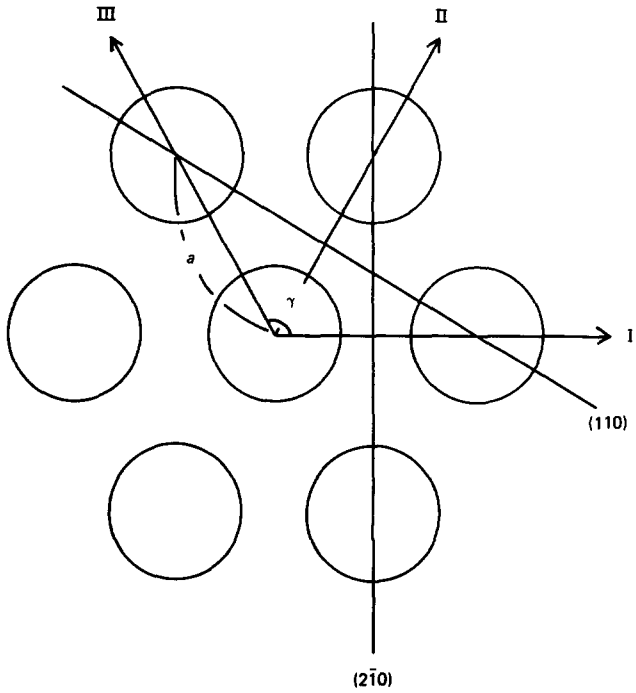

Figure 2 Schematic picture of the chain packing. Conventional unit cell containing one chain stem is used in denoting the planes (2$\bar{1}$0) and (110). The directions [1,0], [1,1], and [0,1] are denoted I, II, and III directions respectively

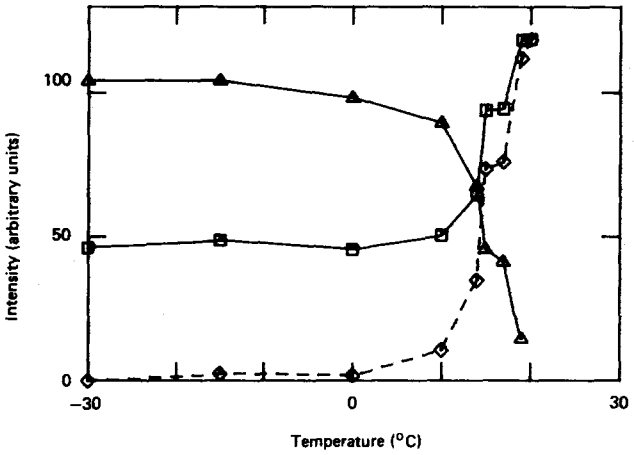

Figure 3 Change with temperature in the integrated intensities of the higher angle (△) and the lower angle (□) peaks in *Figure 1*, and the fraction of the phase IV (◇) estimated by subtracting 0.48 times the intensity of 2$\bar{1}$0 reflection of the phase II from the intensity of the lower angle peak

and IV. Therefore, the spacings determined from the apparent peak positions between 10°C and 19°C are subject to some error. The broken lines in *Figure 4* are the extrapolations of the low temperature data ($T<10$°C) and high temperature data ($T>20$°C). Below 19°C, the two reflections 110 and 2$\bar{1}$0 of the phase II are well separated, indicating that a pseudohexagonal packing of chains with $\gamma<120°$ (γ of about 119.3° at 19°C for example) is maintained up to the vicinity of the transition point. Above 19°C, however, only a single peak of 110 reflection can be observed, which shows a hexagonal packing of the chains with $\gamma=120°$. This sudden change in the chain packing at 19°C clearly demonstrates a first order nature of the transition. *Figure 5* shows the calculated a and γ values by use of the following standard formula,

$$1/d_{hk0}^2=(h^2+k^2-2hk\cos\gamma)/a^2\sin^2\gamma$$

By similar extrapolation of the low temperature data, the values of a and γ of the phase II at 19°C can be estimated as 5.606 Å and 119.32°. It was shown[12,13] and also will be presented in the following section that along the direction II with larger interchain separation lie the chains with the same helical sense. Sudden change of the chain packing at 19°C is a dilatation predominantly transverse to this direction II (*Figure 6*).

A rotational motion of the chains around the chain axes is a specific mode of motion for PTFE above 19°C[7]. The magnitude of the motion below 19°C is of interest in studying the mechanism of the phase transition. *Figure 7* shows a change with temperature in the integrated intensity of a reflection at $2\theta=42.80°$ (from the paper of Weeks[12]) on the second layer line, which must be very sensitive to the rotational motions of the chains. As shown in the Figure, the change in the integrated intensity of the reflection is almost the same as that of the equatorial reflection 2$\bar{1}$0. The decrease in the intensity of the second layer reflection can be explained only by the decrease in the fraction of the phase II; no evident increase in the rotational motion around the chain axis can be detected below 19°C. This fact also supports the simple first order nature of the 19°C transition.

Figure 8 shows a profile of a meridional reflection 0013 observed at 2°C. The reflection is very sharp, giving clear separation of α_1 and α_2 peaks of CuKα, with half width of each peak of about 0.18°. This shows that the intramolecular order is very perfect. Two peaks are

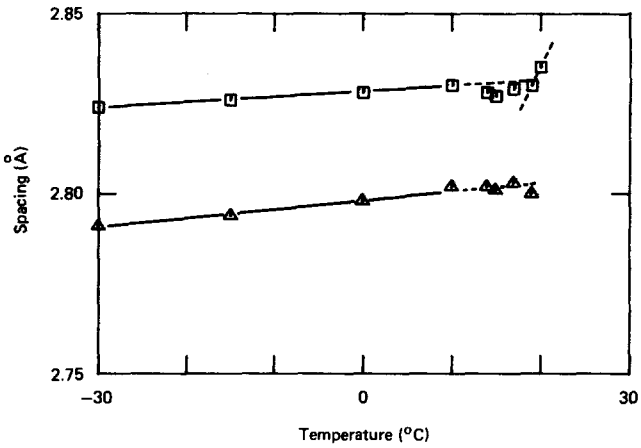

Figure 4 Change with temperature in the apparent spacings d(2$\bar{1}$0)(△) and d(110)(□). Broken lines are the extrapolation from the higher and the lower temperature sides of the transition region

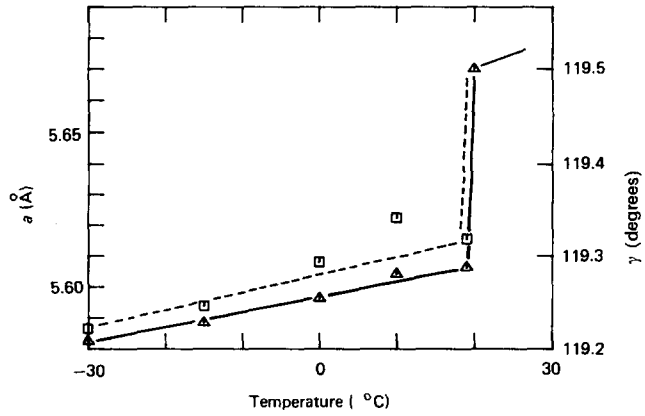

Figure 5 Changes with temperature in the lattice parameters a (△) and γ (□)

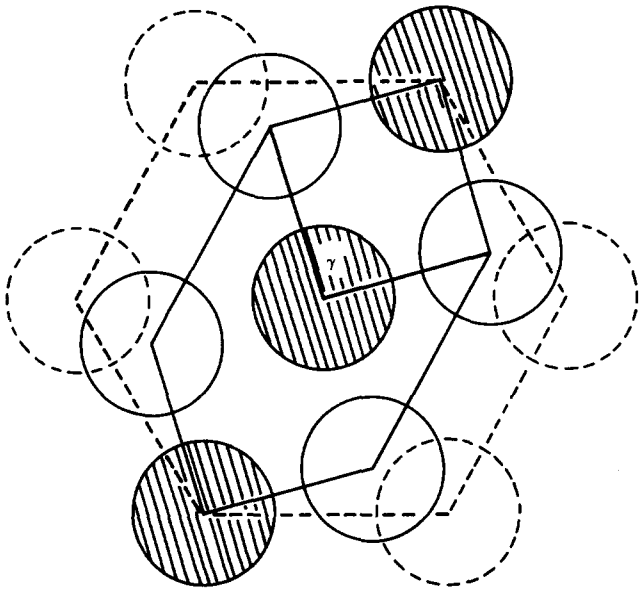

Figure 6 Schematic picture of the change in the chain packing at the 19°C transition. Circles in a solid line represent the positions of the chains before the transition, wheras circles in a broken line represent those after transition. The change in the chain packing is a dilatation predominantly perpendicular to the direction II

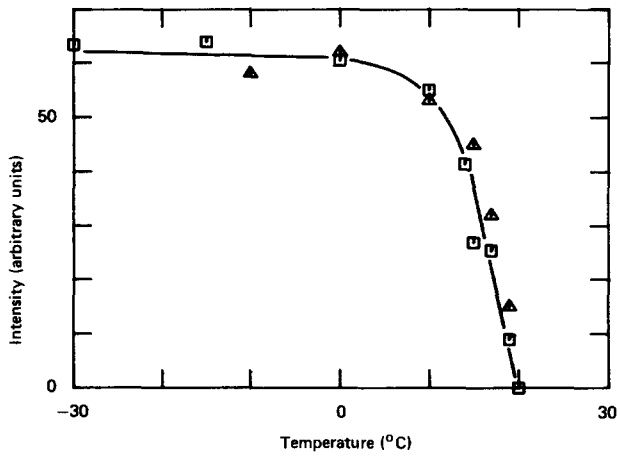

Figure 7 Change in the intensity of a reflection on the second layer line (△), which is compared with that of the 2$\bar{1}$0 reflection (□). Both reflections show quite similar decreases with temperature

separated by the least-squares-method (SALS)[16], and a spacing $d(00l)$ was calculated using $\lambda_{\alpha_1} = 1.54051$(Å) (*Figure 9*). Around 19°C, it gives a sharp increase of about 0.0015(Å), which corresponds well to a conformational change from the 13/6 to 15/7 helix. Further increase in $d(0015)$ above 19°C was shown to be due to an introduction to *trans* bonds in the regular 15/7 helical conformation[11]. The decrease in $d(0013)$ below 19°C, on the other hand, may be due to a departure from the simple 13/6 helical conformation, but at present it is quite uncertain.

Monte Carlo simulation results

It was shown in the previous section that the pseudohexagonal lattice ($\gamma = 119.3°$) of the phase II changes abruptly to the hexagonal lattice ($\gamma = 120.0°$) of the phase IV at 19°C accompanied by the conformation change from the approximately 13/6 helix to the 15/7 helix. The transition is evidently of an order–disorder type. Therefore, what kind of disordering takes place in the high temperature phase IV? We examined the chain packings in the phases II and IV using the MC simulation method.

In our previous paper[14], the crystal structure of the phase II was studied by the MC calculation, where the 13/6 helices were assumed to be packed in a hexagonal lattice ($\gamma = 120°$). The calculation showed a characteristic pattern of linear rows of the chains of the same helical sense in the II and III directions. However, this pattern is not always consistent with the hexagonal lattice; there is no reason for the lattice to be hexagonal. This pattern itself seems to favour the pseudohexagonal lattice ($\gamma \neq 120°$). In fact, the chain packing in the phase II is pseudohexagonal with $\gamma < 120.0°$. We first carried out the

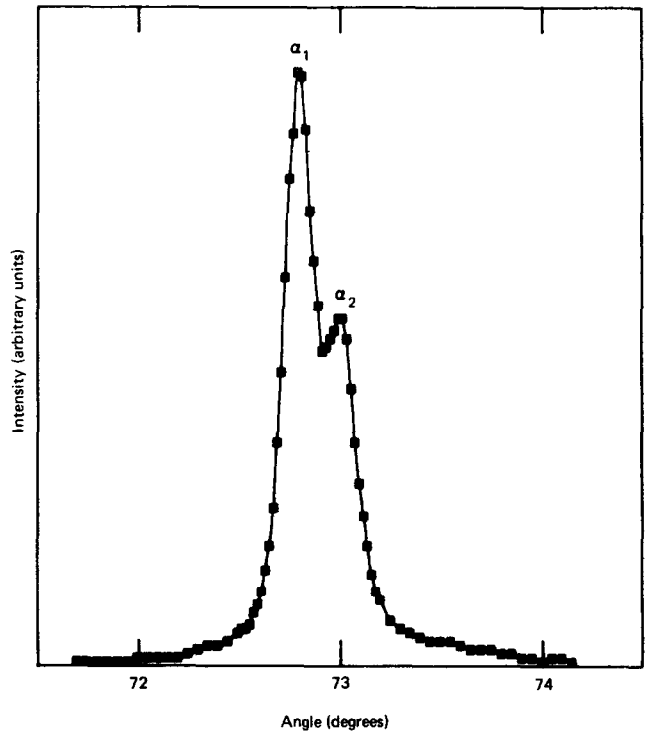

Figure 8 Diffraction profile of the meridional reflection 0013 at 2°C showing clear separation of α_1 and α_2 peaks

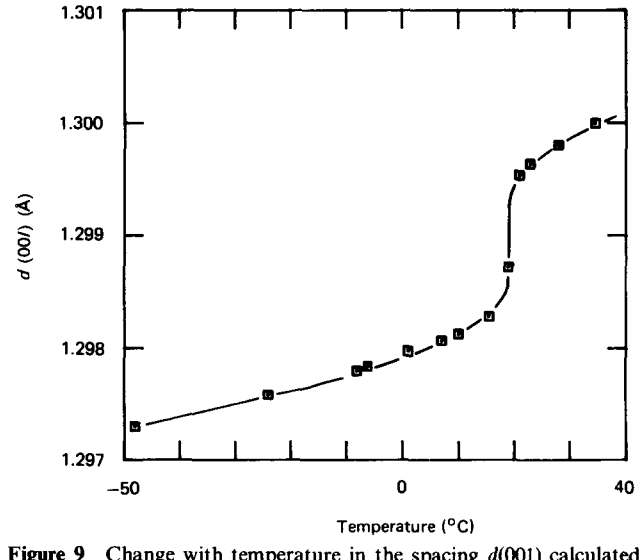

Figure 9 Change with temperature in the spacing $d(001)$ calculated from the peak position of the meridional reflection using $\lambda_{\alpha_1} = 1.54051$ Å

MC calculation of the chain packing in the phase II assuming $\gamma = 119.3°$.

Figure 10 shows results of the MC calculations for the phase II ($\gamma = 119.3°$, $a = 5.65$ Å) at 50K and 300K. At both temperatures, the chains of the same helical sense tend to line up along the direction II. Except for the fact that the rows of the chains of the same helical sense (hereafter referred to simply as the *rows*) along the direction III are less prominent than those along the direction II, the essential feature of the patterns is the same as that of our previous work for the 13/6 helix in the hexagonal lattice[14].

Figure 11 shows the interchain interaction energy between (a) the R-chains, and that between (b) the R-chain and the L-chain, for three different interchain separations. The attractive nature of the interaction is evident between the chains of the opposite helical sense. Since $\gamma < 120.0°$ in phase II, interchain separation along the directions I and III is smaller than that along the direction II. As can be seen in *Figure 10*, the chains of opposite helical sense tend to lie along these I and III directions, which is quite reasonable when we consider the attractive interaction between the chains of the opposite helical sense.

Figure 12 shows detailed orientation patterns at 50K and 300K. Though the arrangements of the R- and L-chains are very ordered, as seen in *Figure 10*, the residual disorder in the chain orientations is remarkable even at 50K.

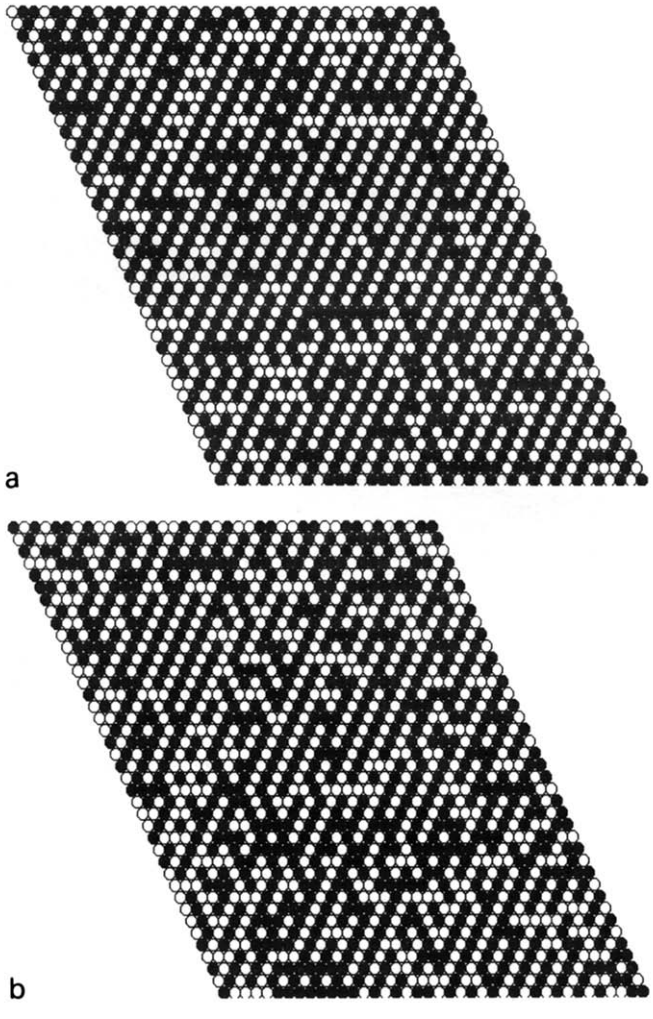

Figure 10 Illustrations of distributions of R(○) and L(●) chains in the phase II at (a) 50K and (b) 300K

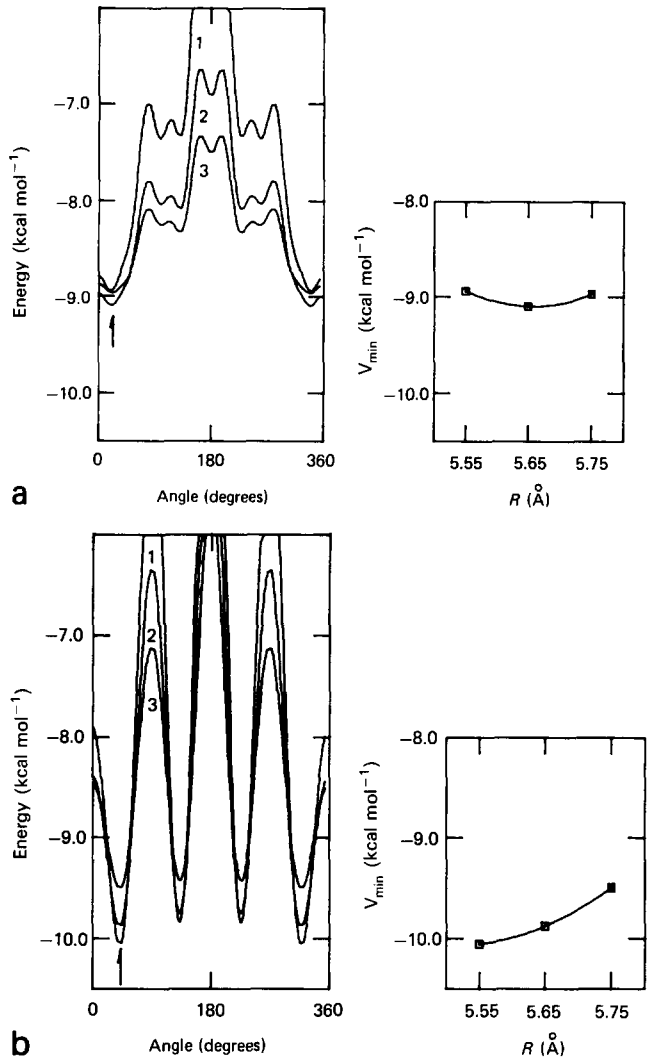

Figure 11 Interchain interaction energy (kcal mol^{-1} of 13 CF_2) between (a) R and R chains, and between (b) R and L chains, each at three different interchain separations (1) $a = 5.55$ Å, (2) $a = 5.65$ Å, (3) $a = 5.75$ Å. The changes with interchain separation in the minimum of the potential (indicated by an arrow), V_{min}, is also shown

The characteristic structure of the rows along the direction II is thus shown to be intimately related to the pseudohexagonal nature ($\gamma < 120.0°$) of the lattice. The 19°C transition with the change in γ from 119.3° to 120.0° must therefore be accompanied with a loss of such a row structure in one direction. *Figure 13* shows a result of the MC calculation for the phase IV ($\gamma = 120.0°$, $a = 5.75$ Å) at 300K. Taking the observed change in the interchain separation of about 0.1 Å at the transition into account, the value of a is assumed as 5.75 Å. It is readily seen that the chain packing in the phase IV is very different from that in the phase II. The tendency for the chains of the same helical sense to line up is also seen in the phase IV. However, the pattern is very disordered in that the rows are very short in comparison with that of the phase II at the same temperature 300K (*Figure 10(b)*).

In the phase IV, it is assumed that the chain takes the 15/7 helical conformation and has the 3_1 symmetry, and that the lattice is hexagonal ($\gamma = 120°$). The interchain interactions in the three directions I, II, and III are, therefore, exactly equivalent. As a result, the obtained pattern has hexagonal symmetry on the average; the rows along the three directions have equal weight. This is again

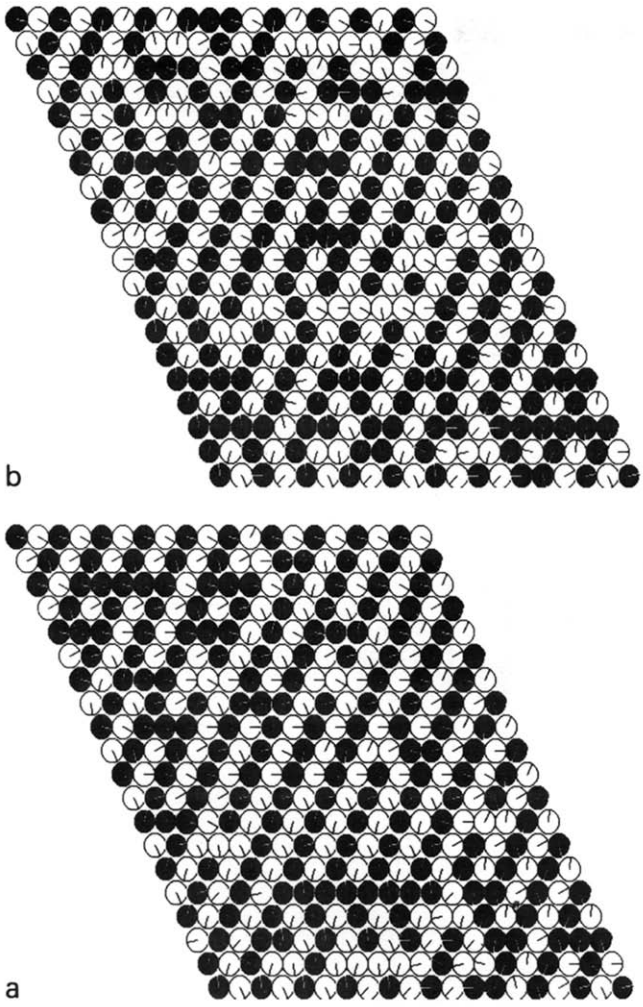

Figure 12 Detailed orientation distributions of chains in a small 20 × 20 portion of the lattice in the phase II at (a) 50K and (b) 300K. The orientations of the chains are represented by the radial lines in the open circles (R chains) and in the filled circles (L chains)

consistent with the hexagonal lattice. This situation is quite a contrast with our previous result of the 13/6 helices in the hexagonal lattice, where the pattern in the hexagonal lattice does not have a hexagonal symmetry[14].

As can easily be seen in *Figure 10*, the like handed chains on the row favour nearly parallel orientations in the phase II. A similar tendency is also seen in the phase IV. However, the short rows hinder growth of the order in the chain interaction along the rows resulting in a disordered orientation distribution (*Figure 14*). The disorder in the phase IV is thus considered to be twofold; one is the disorder in the arrangement of the R- and L-chains, and the other is the disorder in the chain orientations.

Fourier analysis of the pattern in *Figure 13* showed that there still remains some order in the arrangement of the R- and L-chains, which will be lost at still higher temperatures. This behaviour may correspond to a phase transition from the phase IV to phase I or from the phase I to phase I'[1,11].

One important point must be mentioned here. As described in our previous paper[14], the interchain interaction energies, which serve as basic constants in the present MC method, are calculated between the repeating units of the neighbouring chains (13 CF_2 for the phase II and 15 CF_2 for the phase IV). If the motional unit consists of N repeating units, the interchain energies must be multiplied by N, the value of which is unfortunately indefinite at present. The interchain interaction energies appear only through the Boltzmann factor $\exp(-\Delta E/kT)$[14,15], and therefore the uncertainty in the absolute values of the interchain energies is equivalent to the uncertainty in the temperature T. The temperature values of 50K and 300K in the calculation serve only as relative measures of the temperature. When we considered the structure of the phase II in our previous paper[14], we were only interested in its ordered structure. The absolute value of the temperature was not important if we could obtain a well ordered structure. In considering the structure of the phase IV, however, we must treat a degree of disorder itself, which is dependent on temperature. However, since the motional unit is known at present, the temperature value of 300K in the calculation of the phase IV must not be considered to correspond to a real temperature. We must interpret the patterns in *Figures 13* and *14* exhibiting the feature of the

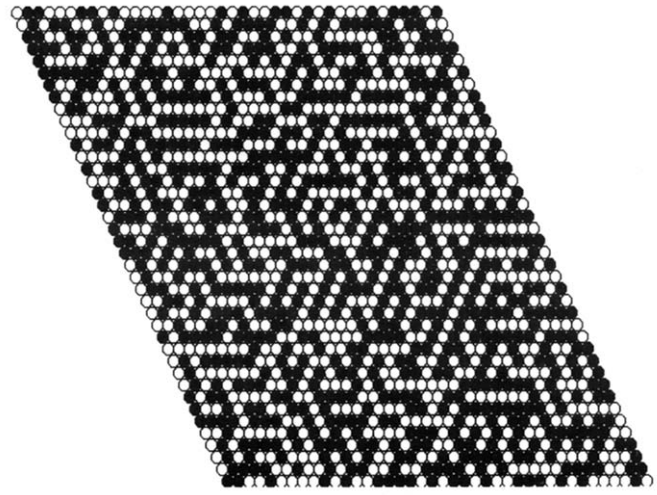

Figure 13 Illustration of distributions of R(○) and L(●) chains in the phase IV at 300 K

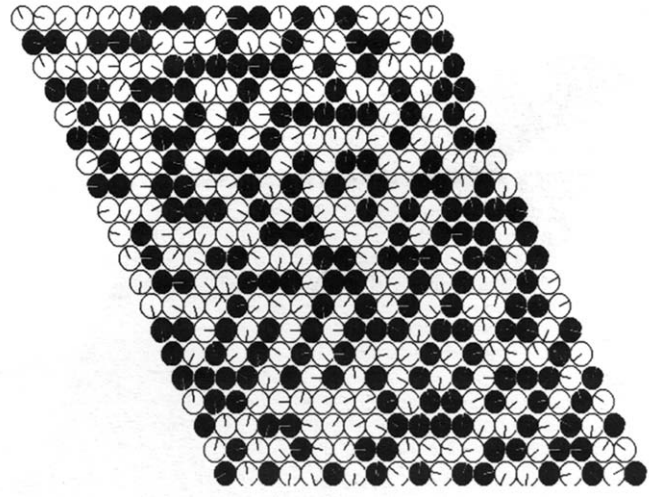

Figure 14 Detailed orientation distribution of chains in a small 20 × 20 portion of the lattice in the phase IV at 300K. The orientations of the chains are represented by the radial lines in the open circles (R chains) and in the filled circles (L chains)

phase IV only qualitatively; we must concentrate on the qualitative differences in the patterns in *Figure 10(b)* and *Figure 13*, which were calculated at the same nominal temperature of 300K.

A similar calculation for the phase IV was done assuming a smaller value of $a = 5.65$ Å. The pattern obtained has the average hexagonal symmetry. However, the pattern is very ordered in that the sizes of the ordered domains are very large. In order to reproduce such a highly disordered structure as is observed by X-ray diffraction, we must use a large value of a such as $a = 5.75$ Å. Therefore, the hexagonal symmetry of the phase IV has its origin in the 15/7 helical conformation and hexagonal lattice, whereas the disorder in the structure comes from a looser chain packing than that in the phase II.

Lastly, the use of slightly larger values of a for both phase II and phase IV should not be taken too seriously. Similar results can be obtained using slightly smaller values of a observed by X-ray diffraction, if we use a slightly higher temperature. But here again we are confronted with the uncertainty in the temperature scale.

REFERENCES

1 Matsushige, K., Enoshita, R., Ide, T., Yamauchi, N., Taki, S. and Takemura, T. *Jpn. J. Appl. Phys.* 1977, **16**, 681
2 Quinn, F. A., Jr., Robert, D. E. and Work, R. N. *J. Appl. Phys.* 1951, **22**, 1085
3 Bunn, C. W. and Howells, E. R. *Nature* 1954, **174**, 549
4 Marx, P. and Dole, M. *J. Am. Chem. Soc.* 1955, **77**, 4771
5 Klug, A. K. and Franklin, R. E. *Faraday Discuss. Chem. Soc.* 1958, **25**, 104
6 Hyndmann, D. and Origlio, G. F. *J. Appl. Phys.* 1960, **31**, 1849
7 Clark, E. S. and Muus, L. T. *Zeit. Krist.* 1962, **117**, 108, 119
8 Hirakawa, S. and Takemura, T. *Jpn. J. Appl. Phys.* 1969, **8**, 635
9 Natarajan, R. and Davidson, T. *J. Polym. Sci. Polym. Phys. Edn.* 1972, **10**, 2209
10 Nicol, M., Wiget, J. M. and Wu, C. K. *J. Polym. Sci. Polym. Phys. Edn.* 1980, **18**, 1087
11 Yamamoto, T. and Hara, T. *Polymer* 1982, **23**, 521
12 Weeks, J. J., Clark, E. S. and Eby, R. K. *Polymer* 1981, **22**, 1480
13 Farmer, B. L. and Eby, R. K. *Polymer* 1981, **22**, 1487
14 Yamamoto, T. *J. Polym. Sci. Polym. Phys. Edn.* 1985, **23**, 771
15 Yamamoto, T. *J. Chem. Phys.* 1985, **82**, 3790
16 Nakagawa, T. and Oyanagi, T. 'Program System SALS for Nonlinear Least-Squares Fitting in Experimental Sciences' in 'Recent Developments in Statistical Inference and Data Analysis', (Ed. K. Matushita), North Holland Publishing Company, 1980, p. 221